

# Spark Ignition of Combustible Gas Mixtures

ERAN SHER

*The Pearlstone Center for Aeronautical Engineering Studies, Department of Mechanical Engineering, Ben-Gurion University of the Negev, Beer Sheva, Israel*

and

JAMES C. KECK

*Department of Mechanical Engineering, Massachusetts Institute of Technology, Cambridge, Massachusetts*

A mathematical model is presented to simulate the evolution with time of a spark channel into a combustion wave. The model considers the phenomena associated with electrical breakdown and arc phases, the plasma conductivity and realistic transport coefficients at high temperatures, and a detailed chemical reaction scheme. The growth of the initial flame radius is calculated by a numerical integration of the model equations and compared with the experimental observation of Tagalian and Heywood.

The time needed for the establishment of a flame propagation in the "like-laminar" regime was found to be strongly dependent on the breakdown energy and on the spark duration, and to a small extent on the initial pressure, temperature, and residual gas fraction. The model was used also to examine quantitatively the effect of some relevant parameters on the cycle-to-cycle variation in the steady-state burning velocity and it was concluded that the cycle-to-cycle variation is attributed mainly either to the inhomogeneity of the trapped mixture and/or to the cycle-to-cycle variation in trapped conditions; a variation of 5% of the volumetric efficiency affects the burning velocity by some  $\pm 13\%$ .

## INTRODUCTION

The cycle-to-cycle variation in a spark ignition engine is primarily dependent on the history of the flame propagation rate from the time of introducing the electrical spark. It was experimentally observed [1, 2] that the manner in which the electrical energy is released dominates the ignition process. The evolution with time of the spark channel into a self-sustained combustion wave is, therefore, a most important process.

Several theoretical works [3-8] have been devoted to investigating the mechanism by which the energy of an electrical discharge is converted into activation energy; however, in parts of them [3-6] the ignition process has been oversimplified by

modeling the ignition source as a hot pocket of burned gases. Kailasanath et al. [7] studied the development of the temperature profile and the effect of the spark-channel radius on the minimum ignition energy of a hydrogen-air mixture. They used a prescribed function for the time-dependent energy deposition in the spark channel, and prescribed function for the time-dependent energy deposition in the spark channel, and assumed a Gaussian profile in space with an increasing characteristic radius. Refael and Sher [8] have presented a mathematical model to simulate the evolution with time of a short segment of spark channel in a combustible mixture. The model assumed an axisymmetric cylindrical flame propagation and electrical conducting column with

moving boundaries. The radial profile of the time-dependent electrical energy input during the arc phase was determined from the calculated plasma conductivity. The present work adopted this model and employed a chemical kinetic scheme for a methane-air mixture. The methane fuel was selected here simply because it is the only alkane fuel for which the chemical kinetics is well known.

The early stage of flame initiation in a spark ignition engine were studied experimentally by several groups. Maly and Vogel [1] examined the ignition of a combustible mixture by using a high energy ignition system in which a large portion of the energy is introduced during the breakdown phase. In these cases a toroidal motion of the gas around the channel axis was observed which affected the time evolution of the ignition process. De-Soete [9] and Gatowki et al. [10] studied the propagation behavior of spark ignited flames during the period of the first 10 ms and later, but in both studies the photographic technique did not allow a close look at the flame development during the first tenths of 1 ms. Tagalian and Heywood [11] measured the flame speed in the very early stages of combustion in an operating, square cross-section cylinder, spark igniton engine. Their important observations seem to support the present predictions.

## THEORETICAL MODEL

The ignition of a combustible mixture by a spark discharge may be considered to proceed in three phases. In the first stage of the breakdown process (10 ns), the electrical potential across the electrode gap is increased until a breakdown on the intervening mixture occurs. Ionizing streams then propagate from one electrode to the other. When a streamer reaches the opposite electrode, the impedance of the gap decreases drastically and the electrical current through the gap increases rapidly. This is associated with a very high temperature rise and a formation of a shock wave. The breakdown phase is then followed by the arc phase ( $\sim .1$  ms) which is characterized by a high electrical current through the mixture while the plasma kernel inflates and endothermic reactions followed by exothermic reactions occur. In the

third phase ( $\sim .2$  ms) the flame front propagation approaches a steady value while the flame thickness increases at a declining rate to reach a steady state value at a later time. The present model simulates the sequence of events during the arc phase and during the very early stages when the combustion wave, which has a cylindrical shape, is formed. The phenomena occurring during the breakdown phase are not considered in detail. However, the results of this phase—the formation of an ionized conducting column and the energy losses by the shock wave—are considered as initial conditions.

## Initial Conditions

Following Maly and Vogel [1], the breakdown phase is characterized by a very high peak value of voltage ( $\sim 10$  kV) and a resultant current of about 200 A for the duration of 1–10 ns. At a very early stage a cylindrical channel of about  $40 \mu\text{m}$  in diameter develops together with a pressure jump and a rapid temperature rise. Maly and Vogel observed that an increase in breakdown energy does not manifest itself at higher kernel temperatures. Instead the channel diameter increases, causing a larger activated gas volume. Refael and Sher [8] showed that the hot plasma at this early stage may be estimated by using a simple approach which assumes that the breakdown energy  $E_{\text{bd}}$  is introduced to the spark channel at a constant volume process during which no significant chemical reactions occur, and that the high pressure which is formed then results in the generation of a shock wave which in turn reduces the pressure of the kernel zone to the ambient pressure and dissipates part of the energy to the surroundings. Since the ratio between the initial temperature of the mixture and the temperature of the spark channel is much smaller than unity, the diameter  $d$  of the cylindrical-shaped channel as formed by this first phase may be estimated by the following expression (Eq. 6, Ref. [8]),

$$d = 2 \left[ \frac{k-1}{k} \cdot \frac{E_{\text{bd}}}{P\pi\delta} \right]^{1/2}, \quad (1)$$

while its temperature is evaluated from  $T_i/k$ ,

where  $T_i$  is the initial temperature of the plasma during the breakdown period (Ref. [11]),  $k$  is the specific heat ratio,  $P$  the chamber pressure,  $\delta$  the electrode gap, and  $E_{bd}$  the energy introduced to the mixture during the breakdown process.

### Electrical Energy Input

The driving function for the model during the arc phase is the resistive heating of the plasma by the electric current. The rate of the heat generation at a segment is determined from Ohm's law by using the expression for electrical conductivity of air at atmospheric pressure as suggested by Plooster [12]:

$$\sigma[\Omega \text{ m}]^{-1} = \frac{4.173 \cdot 10^{-8} \cdot (A_1 + A_2) \cdot T^{-1/2}}{2 \cdot 10^{-15} \cdot (1 - A_1) + A_1 \cdot a_i}, \quad (2)$$

where  $T$  is in  $^{\circ}\text{K}$  and the average electron-ion cross-section  $a_i$  is given by

$$a_i = 2.8 \cdot 10^{-6} \cdot T^{-2} \cdot \left( \frac{A_1 + 3 \cdot A_2}{A_1 + A_2} \right)^2 \cdot \log \frac{1.727 \cdot 10^{-4} \cdot (A_1 + A_2) \cdot T}{(A_1 + 3 \cdot A_2) \cdot (A_1 \cdot \rho)^{1/3}}. \quad (3)$$

In this expression  $A_0$ ,  $A_1$ , and  $A_2$  express the extent to which dissociation, first state, and second state of the ionization process have gone to completion. The present model uses the calculated values for  $A_0$ ,  $A_1$ , and  $A_2$  of Deschambault [13]. The time-dependent boundaries of the plasma are defined, therefore, by the instantaneous field of the temperature which determines the plasma composition and hence the electrical conductivity and the rate of the generated heat. Figure 1 shows some calculated volt-ampere characteristics and the resulting channel growth. The negative slope of the volt-ampere curve, i.e., the current increases as the electrical tension along the arc decreases, is attributed to the increasing of the electrical conductivity of the channel due to its expansion. At the end of the second phase, the electrical tension falls below a critical value, the current is cut, the high temperature of the channel

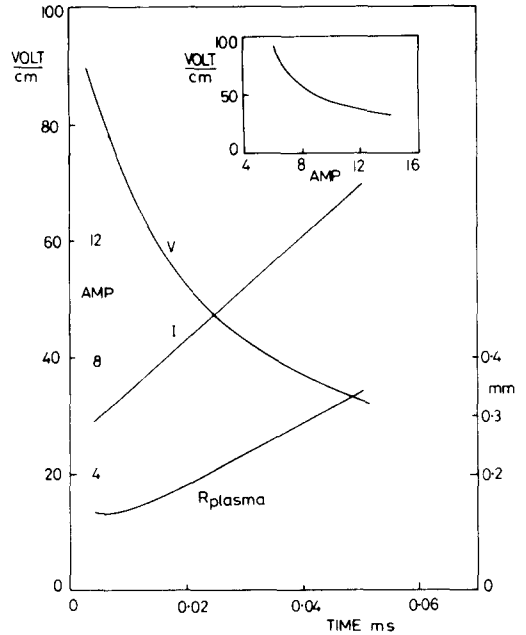


Fig. 1. Some calculated volt-ampere characteristics and the resulting channel growth. Spark duration =  $50 \mu\text{s}$ , breakdown energy =  $.006 \text{ mJ}$ , and the total energy introduced into the intervening mixture =  $6.2 \text{ mJ}$ .

core falls down, and a self-sustained combustion wave is established.

### Mass and Energy Conservation

The sequence of events occurring in the arc and the early growing phases were predicted here by using a similar approach as described by Refael and Sher [8]; the time-dependent profiles (inside and outside the kernel) of the temperature, velocity, and the species concentrations were calculated by solving numerically the general 1-D conservation equation in the following form:

$$\frac{\partial}{\partial t} (\rho\psi) + \frac{1}{r} \frac{\partial}{\partial r} (\rho u\psi) - \frac{1}{r} \frac{\partial}{\partial r} \left( \rho \Gamma_{(\psi)} r \frac{\partial \psi}{\partial r} \right) + s_{(\psi)} = 0, \quad (4)$$

where  $\psi$  is the transported property, which may take the value of 1 for continuity, of the enthalpy for energy conservation or a species concentration for the particular mass conservation.  $\Gamma_{(\psi)}$  and  $s_{(\psi)}$

are the diffusion coefficient and the source term, respectively, associated with the property  $\psi$ ;  $\rho$  is the density;  $u$  is the radial velocity; and  $t$  is the time.

The equations of the model have been transformed into finite-difference equations and solved numerically by a backward difference technique. The domain of solution was a cylinder slice of 10 mm radius and 1 mm height while the finite volume is a simple cell containing a scalar quantity and enclosed by two surfaces of constant  $r$  separated by .02 mm. A time increment of  $10^{-8}$  s was used for the numerical integration. For more details on the mathematical formulation of the finite-difference equations and the technique adopted for solution, the reader is referred to Sher and Refael [8] and Sher [14].

### Chemical Kinetics

A number of kinetic schemes to model methane/air flames have been proposed in the literature. A fairly comprehensive model has been suggested by Warnatz [15] in which 23 species and 58 reaction steps were considered. In the present work the complete scheme of Warnatz was used to model the growth and establishment of the initial flame. However, it is interesting to note that much effort has been spent to trace the most important path through which the methane oxides under the particular conditions of the present problem (initiation and oxidation at high temperature). A systematic study, which is not the subject of the present work, suggested that a simplified reaction scheme which includes 14 species and 17 reaction steps (Fig. 2) still does a good job of reproducing the time-dependent profiles of the significant species, as well as the establishment of the steady burning velocity. The details of this study are reported in Ref. [16].

### Equation of State and Transport Coefficients

Since the calculations of the electrical conductivity and the generated heat by chemical transformation imply a knowledge of the composition of the mixture and its state, the model requires fairly realistic equations of state and transport coeffi-

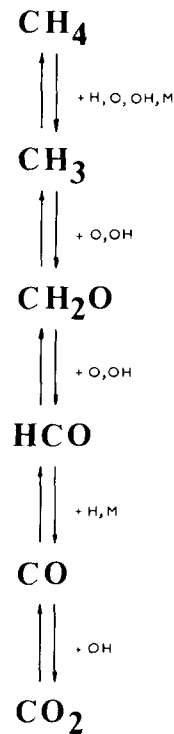


Fig. 2. The adapted mechanism of  $\text{CH}_4$  oxidation at high temperatures [16].

icients. However, due to the lack of information in experimental measurements at high temperatures, on the one hand, and formulating the partition function of the various species involved, on the other hand, and due to the problem conditions which limit the mass fraction of the molecules which contain C atoms to about 6%, the present model uses the thermophysical properties of pure air and assumes a Lewis number equal to 1. Following Plooster [12], the thermal conductivity was determined by

$$K \text{ [kW/m } ^\circ\text{K]}$$

$$\begin{aligned}
 &= 10^{-5} \cdot (1 - A_1) \cdot T^{1/2} + 14.88 \cdot 10^{-12} \\
 &\cdot \sigma \cdot T + 220 \cdot \rho \cdot dA_0/dT, \quad (5)
 \end{aligned}$$

where the three terms express the contributions of the neutral particles, the electrons, and the diffusion of recombination energy, respectively. The binary molecular diffusion coefficient between one particular species and the mixture was estimated

by

$$D_{im} = D_{m,m} \sqrt{M_m/M_i}, \quad (6)$$

where  $D_{m,m}$  was derived from the thermal conductivity, specific heat capacity, and the density, while the compressibility factor and the specific heat capacity were calculated by using the approach of Landolt-Bornstein [17] for pure air. The latter was derived by differentiating the classical enthalpy function, which includes the energy contribution of the molecules, atoms, electrons, dissociation, and both the first and the second states of ionization.

**RESULTS**

**General Characteristics of the Early Growth Phase**

Figure 3 compares some characteristics of a typical ignition process with those of a thermal wave. The thermal wave has been produced by introducing an identical spark into a nonreactive medium. The position of the flame front as well as the position of the thermal wave were defined as the radial distance at which the first (from outside) temperature gradient reaches a local maximum

value. The flame (or the thermal wave) thickness,  $\delta^*$ , was defined by

$$\delta^* = \frac{T_{ad} - T_u}{(\partial T / \partial r)_{max}} \cdot \frac{1}{\alpha / u_{b0}} \quad (7)$$

(for a thermal wave,  $T_{ad}$  corresponds to  $T_{ad}$  for stoichiometric mixture of  $CH_4$ -air at standard conditions), and  $E^*$ , the cumulative heat released by chemical reactions, was defined by

$$E^* = \int_0^t \int_0^R \dot{E}_{chem} \cdot \rho \cdot r \cdot dr \cdot dt / E_{spark}. \quad (8)$$

The flame front distance seems to increase rapidly during the arc period ( $t < .05$  ms), while endothermic reactions dominate the combustion to produce hydrogen, oxygen, and hydroxide radicals, and then reaches a steady value after a relatively short time of about .2 ms. Meanwhile the flame thickness seems to increase at a declining rate to approach its steady value at a later time  $> 1$  ms; this is associated with the decreasing of the postflame temperature to its adiabatic value at a comparable rate. During the period in which endothermic reactions are dominant (in the reactive medium), the thermal wave seems to travel faster than the flame front, decelerates to zero

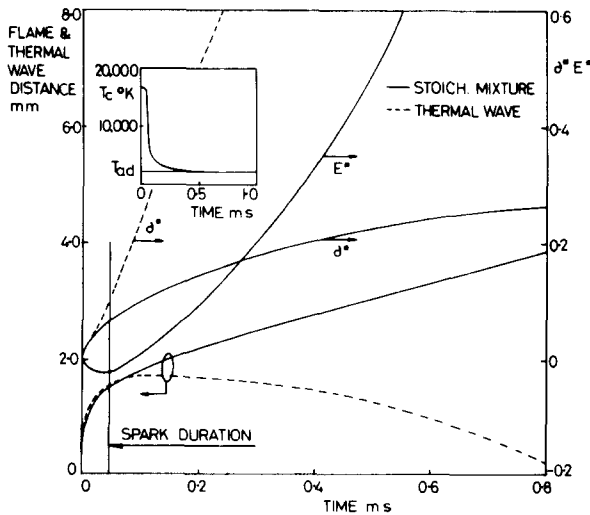


Fig. 3. Some characteristics of a typical ignition process. Total introduced energy ( $E_{spark}$ ) = .484 mJ, and  $E_{td}$  = .008 mJ.

velocity, and then travels backward as the cylinder core cools down due to outward heat conduction.

Systematic calculations showed that the initial growing time of the flame (before steady-state propagation is established) is strongly dependent on the equivalence ratio, breakdown energy, and spark duration, and only to an insignificant extent on the initial pressure (5–20 A), temperature (350–540K), and the residual gas fraction (.05–.2).

### The Effect of Equivalence Ratio

A shift from a stoichiometry condition results in a longer time for the establishment of the steady flame velocity together with a significant change in the period in which endothermic reactions dominate (Fig. 4). In lean mixtures, the fuel concentration is low and the production rate of the initiative radicals throughout  $\text{CH}_4 + \text{M} \rightarrow \dot{\text{C}}\text{H}_3 + \dot{\text{H}} + \text{M}$  followed by  $\text{O}_2 + \dot{\text{H}} \rightarrow \text{OH} + \dot{\text{O}}$ , etc., is low. Also, the low concentration of the fuel reduces the probability of being attacked by these radicals, and higher radical concentrations must be built up to establish a self-sustained combustion wave. In rich mixtures, the high monoxide concentration enhances the significance of some reverse reactions and affects the time for chemical equilibrium accomplishment. Far from stoi-

chiometric conditions a few milliseconds were needed to establish a steady-state propagation.

### The Effect of Breakdown Energy and Spark Duration

Curve 2 in Fig. 5 shows the early growth of a typical ignition process. An increase in the spark duration (curve 3) requires a longer period of a very high back-flame temperature together with a further inflation of the spark channel (Fig. 1) and thus contributes to a slower deceleration of the flame front. In this case the flame front travels a longer distance during the first .2 ms, and then reaches a steady-state propagation in a shorter time for which the probability of initiating a self-sustained combustion wave in nonhomogeneous mixtures is high. A decrease in the spark duration (curve 1) results in a faster deceleration of the flame front at a very early stage, and may lead to ignition failure. However, in this case the flame recovered after .25 ms, and reached a steady propagation. For the same spark duration of .01 ms, an increase in the breakdown energy (curve 4) can significantly improve the ignition process; the initial diameter of the spark kernel (after the breakdown phase) is higher [Eq. (1)] and again a large volume of hot region is formed in a short time. In general, Fig. 5 suggests that introducing a

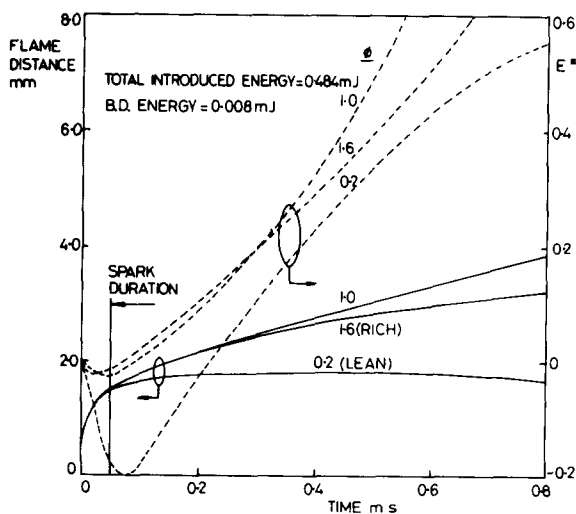


Fig. 4. The effect of the equivalence ratio on the early growth phase.

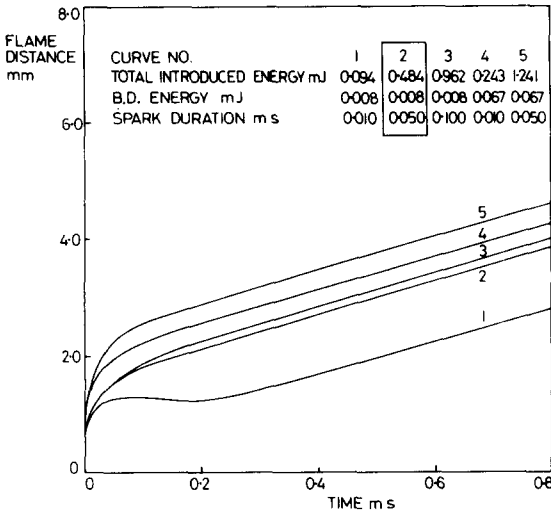


Fig. 5. The effect of breakdown energy and spark duration on the early growth phase.

higher energy during the breakdown phase and a longer spark duration contribute to the creation of a larger volume of hot region in a short time.

**Application to Spark Ignition Engines**

Tagalian and Heywood [11] measured the flame speed in the very early stages of combustion in an operating spark ignition engine. The engine had a square cross-section and two parallel walls of quartz, allowing visualization of the entire combustion chamber. The engine was operated at 1500 rpm and .5 A intake pressure, and used a premixed propane-air mixture with a fuel-air equivalence ratio of .9. Using the z-Schlieren technique, high-speed movies of about one frame per crank angle degree were taken (1 crank angle degree = .12 ms). Their results are replotted in Fig. 6. The authors found that the flame starts from a smooth-surfaced spherical kernel about 1 mm in diameter which is formed during the first crank angle degree and then the flame radius increases linearly with time over the first 15°, where  $dr/dt$  is essentially constant but shows a scatter of  $\pm 20\%$  from cycle to cycle.

The present study (Figs. 3-5) suggests that the very early stages of a spark ignited flame, the steady-state establishment occurs merely in the

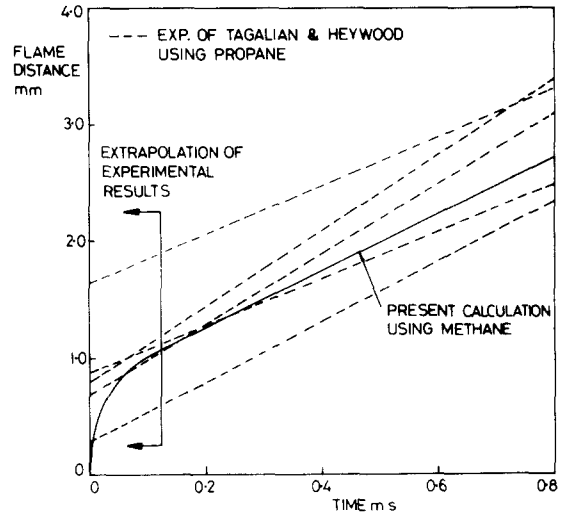


Fig. 6. Replotted experimental observations of Tagalian and Heywood [11], and a predicted curve from the present study.

first few .1 ms, or even faster for this particular experiment (Fig. 6), and the observed "like-laminar" regime which follows this period where the flame radius increases linearly with time is fully confirmed. However, the extrapolation of the experimental results to the very early stage (before .12 ms) may not be entirely correct. The present calculated curve shown in Fig. 6 has been predicted by using the estimated experimental conditions in Table 1, column 2. This set of conditions resulted in a steady-state curve slope which is very close to the average slope observed. However, its vertical position was fitted to the experimental results by selecting a reasonable set of spark characteristics ( $E_{bd} = .01$  mJ and spark duration = .05 ms), as these have not been reported by Tagalian and Heywood. Figure 5 suggests that a slightly different set may have drastically changed the plane position of this curve, which may be a plausible explanation for the scattering observed. The different slopes observed at different cycles are probably attributed either to the inhomogeneity of the trapped mixture and/or to the cycle-to-cycle variation in trapped conditions. Table 1 illustrates the effect of a possible variation in each parameter on the steady-state burning velocity. A variation of 5% of the volumetric efficiency (= 1 minus the residual gas fraction) seems to affect significantly

TABLE I

The Effect of Various Parameters on the Steady-State Burning Velocity of a Propagation Combustion Wave in SI Engine (the Estimated Experimental Conditions Are Related to the Study of Tagalian and Heywood [11])

$\psi$	Experimental Conditions	Possible Variation	$U_b(\text{at } \psi \pm 5\%)/U_{b0} - 1$						
			$(U_{b0} = 53.9 \text{ cm/s})$						
			-0.3	-0.2	-0.1	+0.1	+0.2	+0.3	
Pressure (atm)	2.4	+5%							
		-5%							
Temperature (K)	480	+5%							
		-5%							
Equivalence ratio	0.90	+5%							
		-5%							
Volumetric efficiency	0.82	+5%							
		-5%							
Extreme Conditions		Higher $U_b$							
		Lower $U_b$							

the burning velocity by 13%, while similar variations in the temperature and equivalence ratio affect the burning velocity by 10% and 5%, respectively. Extreme conditions which may reflect the effect of in-cylinder inhomogeneity together with a cycle-to-cycle variation result in an estimated deviation of 30%. It is interesting to note that excluding the predicted effect of the spark characteristics on the initial volume of the hot region, and hence the position of the flame growth curve, the simple empirical expression of Metghalchi and Keck [8] (for the prediction of the burning velocity of propane) does predict a very similar dependence and hence leads to very similar conclusions about the possible sources and magnitude of errors.

## CONCLUSIONS

A mathematical model was presented to simulate the evolution with time of a spark channel into a combustion wave. The establishment period of the flame growth was studied and the following conclusions have been drawn.

1. It was recognized that a better spark would

produce a larger volume of hot region in a shorter time for which the probability of initiating a self-sustained combustion wave in nonhomogeneous mixtures is higher.

2. The initial growing time of the flame is strongly dependent on the equivalence ratio (longer time for off-stoichiometric mixtures), on the breakdown energy, and on the spark duration.
3. The predicted time for the establishment of a flame propagation and the steady-state propagation rate was found to be in qualitative agreement with experimental observations.
4. The model suggests some possible explanations for the cycle-to-cycle variation in the dimension of the initial hot region created, as well as in the steady-state burning velocity, and estimates the deviation by  $\pm 30\%$ .

## NOMENCLATURE

$A_0, A_1, A_2$  the extent to which dissociation, first state, and second state of ionization process have gone to completion

$a_i$	average electron-ion cross-section diameter
$D_{i,m}$	binary molecular diffusion coefficient
$d$	diameter
$E_{bd}$	energy introduced to the mixture during the breakdown phase
$\dot{E}_{chem}$	rate of heat released by chemical reactions per unit mass
$E_{spark}$	total energy introduced to the inter-vening mixture
$E^*$	cumulative heat released by chemical reactions [Eq. (5)]
$k$	specific heat ratio
$\delta$	gap between electrodes
$M_i$	molecular weight of species $i$
$P$	pressure
$R$	radius
$r$	radial coordinate
$S(\psi)$	source term associated with the property $\psi$
$T$	temperature
$T_{ad}$	flame adiabatic temperature
$T_c$	temperature at the kernal axis ( $r = 0$ )
$T_u$	temperature of unburned mixture
$t$	time
$U_b$	burning velocity
$U_{b0}$	burning velocity for the conditions of Table 1, column 2

### Greek Symbols

$\alpha$	thermal diffusivity
$\Gamma(\psi)$	transport coefficient associated with the property $\psi$
$\delta^*$	the flame or thermal wave thickness [Eq. (4)]
$\rho$	density
$\sigma$	electrical conductivity
$\phi$	equivalence ratio
$\psi$	general dependent transported property

*The first author would like to express sincere appreciation to the members of the Sloan Automotive Laboratory at MIT for providing the facilities for this research and for the extremely invaluable discussions during the laboratory seminars. The author is also indebted to the directors of the Energy Laboratory at MIT for providing a supporting grant.*

### REFERENCES

1. Maly, R., and Vogel, M., *Seventeenth Symposium (International) on Combustion*, The Combustion Institute, 1978, p. 821.
2. Ballal, D. R., and Lefebvre, A. H., *Combust. Flame* 24:99-108 (1975).
3. Overley, J. R., Overholser, K. A., and Reddien, G. W., *Combust. Flame* 31:69-83 (1978).
4. Akindale, O. O., Bradley, D., Mak, P. W., and McMahon, M., *Combust. Flame* 47:129-155 (1982).
5. Sher, E., Accepted for publication by the *Israel J. of Tech.* (1985).
6. Sher, E., and Refael, S., *Nineteenth Symposium (International) on Combustion*, The Combustion Institute, 1982, p. 251.
7. Kailasanath, K., Oran, E., and Boris, J., *Combust. Flame* 173-190 (1982).
8. Refael, S., and Sher, E., *Combust. Flame* 59:17-30 (1985).
9. De-Soete, G. C., *Combustion in Engineering*, Vol. 1., p. 93, 1983.
10. Gatowski, J. A., Heywood, J. B., and Deleplace, C., *Combust. Flame* 56:71-81 (1984).
11. Tagalian, J., and Heywood, J. B., Accepted for publication by *Combust. Flame* (1985).
12. Plooster, M. N., *Phys. Fluids* 14:2111-2123 (1971).
13. Deschambault, R., Ph.D. Thesis, Univ. of Toronto Institute for Aerospace Studies, 1980.
14. Sher, E., *Combust. Flame* 47:109-128 (1982).
15. Warantz, J., *Eighteenth Symposium (International) on Combustion*, The Combustion Institute, 1980, p. 369.
16. Keck, J. C., and Sher, E., in preparation.
17. Landolt-Bornstein, *Zahlenwerte und Funktionen*, Vol. 2, Part 4, Springer-Verlag, 1961.
18. Metghalchi, M., and Keck, J. C., *Combust. Flame* 143-154 (1980).

*Received 13 August 1985; revised 23 April 1986*